4828 *Inorg. Chem.* **1995,** *34,* 4828−4835

Di-, Tri-, and Tetranucleating Pyridyl Ligands Which Facilitate Multicenter Magnetic Exchange between Paramagnetic Molybdenum Centers

Angelo J. Amoroso, Alexander M. W. Cargill Thompson, John P. Maher, Jon A. McCleverty,* and Michael D. Ward*

School of Chemistry, University of Bristol, Cantock's Close, Bristol, BS8 1TS, U.K.

Received April 20, 1995[⊗]

Two series of di-, tri- and tetranucleating bridging ligands have been prepared comprising 4-pyridyl binding sites radiating out from a central aromatic core, linked by ethenyl (series **A**) or ethynyl (series **B**) conjugated spacers. All of the ligands were prepared by a simple one-pot Heck coupling reaction between 4-vinylpyridine (series **A**) or 4-ethynylpyridine (series **B**) and the appropriate polybromobenzene. Complexes with these ligands were prepared by attachment of paramagnetic {Mo(NO)Tp*Cl} fragments to some or all of the pyridyl binding sites of the ligands. Electrochemical studies showed that (i) the redox splitting $\Delta E_{1/2}$ between the 17-electron/18-electron couples of the Mo centers varies with the substitution pattern of the bridging ligand, such that *ortho* and *para* relationships between two {Mo(NO)Tp*Cl} fragments result in stronger interactions than a *meta* relationship and that (ii) ligand series **A**, with ethenyl spacers between the pyridyl termini and the central aromatic ring, gives slightly stronger electrochemical interactions than does ligand series **B**, which contains ethynyl spacers. EPR spectra showed that in all complexes of nuclearity two or more, magnetic exchange between the unpaired electrons is occurring; i.e., all unpaired electrons apparently couple to all molybdenum nuclei. The triangular trinuclear complexes and rectangular tetranuclear complexes represent the first examples of well-defined complexes where multicenter magnetic exchange is unequivocally apparent from the EPR spectra.

Introduction

The availability of a wide range of ligands which can bridge two or more remote metal centers has been of fundamental importance in recent coordination chemistry. Such bridging ligands allow the preparation of polynuclear complexes in which long-range metal−metal interactions in all their forms may be studied, such as optical electron-transfer in mixed valence species,[1] photoinduced electron transfer or energy transfer between an excited-state chromophore and a quencher,[2] and magnetic exchange between paramagnetic centers.[3] Current applications of such bridged polynuclear complexes span the whole range of chemistry from theoretical to biomimetic, including areas such as new magnetic materials and solar energy conversion.

The vast majority of bridging ligands are dinucleating: pyrazine and 4,4′-bipyridine are archetypal examples. In contrast, ligands which contain three or more binding sites radiating out from a central core, and which can therefore potentially bind three or more metal ions in a polygonal array, are relatively rare.[4,5] Two interesting recent examples are hexakis(4-pyridyl)benzene (L^1)[5a] and 1,3,5-tris(4′-terpyridinyl)benzene (L^2).[4a] Such multinucleating ligands are of interest for several reasons. Not only will they permit extension of the various studies of metal−metal interactions to higher nuclearity systems, but they may also serve as a starting point for metal-containing arborols and two-dimensional networks. In addition, it has recently been shown that, since molecules with 3-fold symmetry or higher may be octapolar, their non-linear optical properties are of interest.[6] In this paper we describe a simple, general, synthetic route based on the Heck reaction[7] to a series of bridging ligands which contain two, three, or four pyridyl ligands radiating out from a central phenyl ring (Figure 1). Complexes of these ligands with paramagnetic {Mo(NO)-Tp*Cl} [Tp* = hydrotris(3,5-dimethylpyrazolyl)borate] end-groups provide systems in which magnetic exchange interactions between two, three and four paramagnetic centers can be unequivocally established by EPR spectroscopy. A preliminary communication describing part of this work has been published.[8]

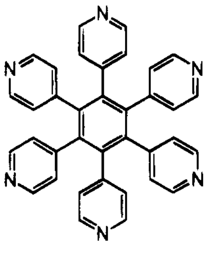

L^1

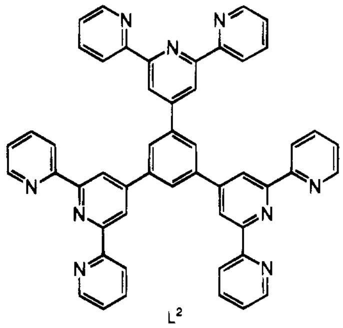

L^2

[⊗] Abstract published in *Advance ACS Abstracts,* September 1, 1995.

(1) (a) Ward, M. D. *Chem. Soc. Rev.* **1995**, 121. (b) Kalyanasundaram, K.; Nazeeruddin, M. K. *Inorg. Chim. Acta* **1994**, *226*, 213.

(2) (a) Sauvage, J.-P.; Collin, J.-P.; Chambron, J.-C.; Guillerez, S.; Coudret, C.; Balzani, V.; Barigelletti, F.; De Cola, L.; Flamigni, L. *Chem. Rev.* **1994**, *94*, 993. (b) Balzani, V.; Scandola, F. *Supramolecular Photochemistry*; Ellis Horwood: Chichester, U.K., 1991.

(3) (a) Kahn, O. *Molecular Magnetism;* VCH Publishers, Inc.: New York, 1993. (b) Das, A.; Maher, J. P.; McCleverty, J. A.; Navas Badiola, J. A.; Ward, M. D. *J. Chem. Soc., Dalton Trans.* **1993**, 681.

(4) (a) Constable, E. C.; Cargill Thompson, A. M. W. *J. Chem. Soc., Chem. Commun.* **1992**, 617. (b) Baxter, P.; Lehn, J.-M.; De Cian, A.; Fischer, J. *Angew. Chem., Int. Ed. Engl.* **1993**, *32*, 69.

(5) (a) Breslow, R.; Crispino, G. A. *Tetrahedron Lett.* **1991**, *32*, 601. (b) Pugh, C.; Percec, V. *J. Mater. Chem.* **1991**, *1*, 765.

(6) Verbiest, T.; Clays, K.; Samyn, C.; Wolff, J.; Reinhoudt, D.; Persoons, A. *J. Am. Chem. Soc.* **1994**, *116*, 9320.

(7) Heck, R. F. *Org. React.* **1981**, *27*, 345.

(8) Amoroso, A. J.; Maher, J. P.; McCleverty, J. A.; Ward, M. D. *J. Chem. Soc., Chem. Commun.* **1994**, 1273.

0020-1669/95/1334-4828$09.00/0

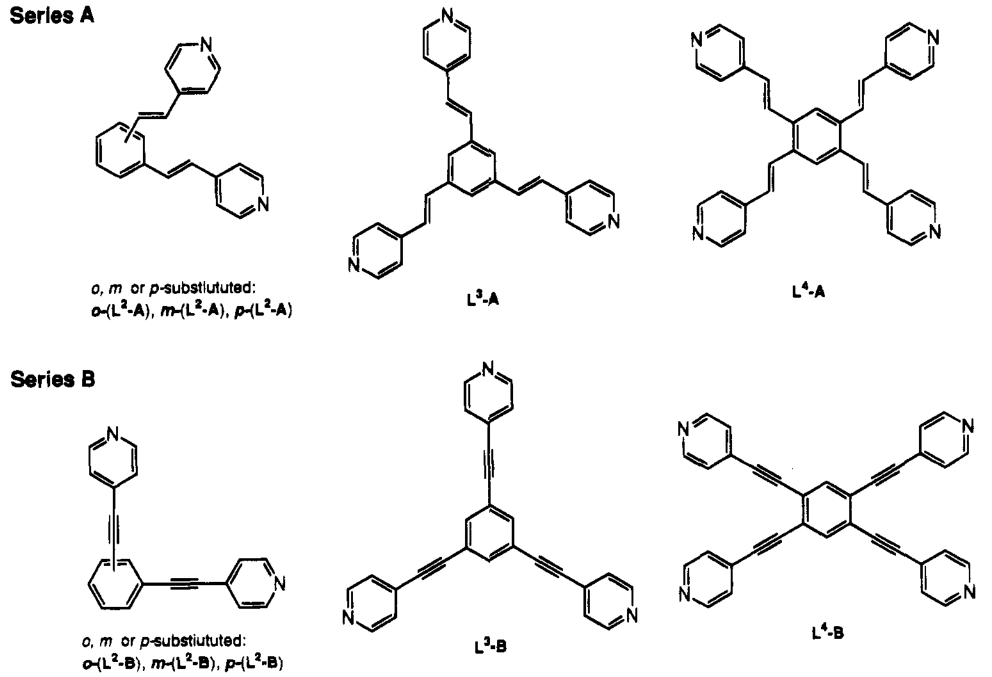

Figure 1. Structure of the ligands described in this paper, showing the labeling scheme used.

Experimental Section

General Details. The following instruments were used for routine spectroscopic and electrochemical work: ^{1}H NMR spectroscopy, Jeol GX-270 or GX-400 spectrometer; electron-impact (EI) and fast-atom bombardment (FAB) mass spectrometry, VG-Autospec; EPR spectrometry, Bruker ESP-300E; UV−vis spectrophotometry, Perkin-Elmer Lambda 2; FT-IR spectrometry, Perkin-Elmer 1600. Electrochemical experiments were performed with a PC-controlled EG&G-PAR model 273A potentiostat, with Pt-bead working and counter electrodes and an SCE reference, using CH_2Cl_2 as solvent containing 0.1 mol dm^{-1} [^{n}Bu$_4$][PF$_6$]. All reagents and starting materials were obtained from commercial sources (Aldrich, Lancaster, Avocado) and used as received. Solvents for reactions and electrochemistry were predried. 4-Ethynylpyridine[9] and [Mo(NO)Tp*Cl$_2$][10] were prepared by the published methods.

Preparations of Ligands. All of the ligands were prepared in the same manner by reaction of the appropriate polybromobenzene, *ca.* 1.25 equiv of 4-vinylpyridine or 4-ethynylpyridine *per* aromatic bromine substituent, and a catalytic amount (*ca.* 10 mol %) of Pd(OAc)$_2$ and PPh$_3$, in dry Et$_3$N at 100 °C under N$_2$. The details given here for preparation of **L^3-B** are representative. A mixture of 1,3,5-tribromobenzene (0.63 g, 2.0 mmol), 4-ethynylpyridine (0.80 g, 7.7 mmol, 1.28 equiv *per* aromatic bromine substitutent to be replaced), palladium(II) acetate (0.014 g, 0.11 mmol) and PPh$_3$ (0.032 g, 0.12 mmol) was placed in a N$_2$-purged Schlenk tube. Dry Et$_3$N (1 cm^3) was added, the tube sealed, and the mixture heated to 100 °C with stirring for 3 days. After cooling, the solid dark mass was dissolved in CH_2Cl_2 (200 cm^3) and extracted thoroughly with water (3 x 150 cm^3). The residual organic phase was dried (MgSO$_4$), concentrated *in vacuo*, and chromatographed over neutral alumina (Brockmann activity III) using 1−2% EtOH in CH_2Cl_2. Traces of unreacted 4-ethynylpyridine eluted first, followed by 1,3,5-tris(4-pyridylethenyl)benzene (**L^3-B**) as a pale yellow band. Evaporation to dryness followed by recrystallization from MeOH/H$_2$O afforded pure **L^3-B** as an off-white crystalline solid (58% yield).

The other ligands were prepared by an essentially identical method, the only differences being in the method of purification of the crude compounds after extraction of the reaction mixture with CH_2Cl_2. These are as follows. *o*-**L^2-B**, *m*-**L^2-B**, and *p*-**L^2-B** were purified by repeated chromatgraphy on activity III alumina with CH_2Cl_2 containing 1% (v/v) EtOH. **L^4-B** was not chromatographed due to its low solubulity; after the reaction, the solid mass was suspended in CH_2Cl_2 (150 cm^3) and treated with ultrasound (cleaning bath) to break up the material and then filtered. The filtrate was concentrated *in vacuo* and cooled and the solid product filtered off; it was finally recrystallized from boiling CHCl$_3$. The **A**-series ligands, which were obtained in much higher yields than the **B**-series ligands, were isolated quite pure from the reactions. The crude CH_2Cl_2 extracts were evaporated to dryness, and the crude solids were then washed with ether in an ultrasound cleaning bath and then recrystallized from acetone or ethanol/H$_2$O.

Details of ^{1}N NMR, mass spectrometric, and analytical data and yields for the ligands are given in Tables 1 and 2.

Preparations of Molybdenum Complexes. Again, the preparations are all very similar and the method described below for complexes of **L^3-B** is typical. A mixture of **L^3-B** (0.10 g, 0.26 mmol), [Mo(NO)-Tp*Cl$_2$] (0.65 g, 1.32 mmol, 1.7 equiv *per* pyridyl binding site) and dry Et$_3$N (3 cm^3) in dry toluene (100 cm^3) under N$_2$ was heated to reflux for 3 days. Additional portions of [Mo(NO)Tp*Cl$_2$] (5 x 0.10 g, total 1.0 mmol) were added to the mixture approximately every 12 h. After concentration to dryness *in vacuo*, the residue was chromatographed over silica. Initially elution with CH_2Cl_2 removed unreacted [Mo(NO)Tp*Cl$_2$] (orange) and the byproduct [{Mo(NO)Tp*Cl}$_2$(μ−O)] (very pale green). The solvent polarity was then increased steadily by addition of increasing amounts of thf to the CH_2Cl_2 used as eluent, until the complexes eluted in the order **Mo$_3$(L^3-B)** (1% THF in CH_2Cl_2), **Mo$_2$(L^3-B)** (CH_2Cl_2/THF, 9:1 v/v) and finally **Mo(L^3-B)** (CH_2Cl_2/THF, 1:1 v/v) as well-separated dark bands. In each case the fraction was evaporated *in vacuo* and then reprecipitated from CH_2Cl_2/hexane (1:1, v/v) by reduction in volume. The dark solids were filtered off, washed with hexane, dried, and stored under N$_2$. The purities of the inidividual compounds were checked by TLC, and they were rechromatographed if necessary.

A summary of the experimental details (chromatography conditions, yields), mass spectroscopic data and elemental analyses for the complexes is given in Table 3.

Results and Discussion

Ligand Syntheses. The Heck reaction,[7] involving coupling of 4-vinylpyridine (ligand series **A**) or 4-ethynylpyridine (ligand series **B**) with a polybromobenzene in the presence of Pd(OAc)$_2$/PPh$_3$ as catalyst, proved to be a simple one-step synthetic route to all of the ligands. This is a potentially general method for preparing a variety of new polynucleating ligands that is limited

---

(9) Ciana, L. D.; Haim, A. *J. Heterocycl. Chem.* **1984**, *21*, 607.

(10) (a) Jones, C. J.; McCleverty, J. A.; Reynolds, S. J.; Smith, C. F. *Inorg. Synth.* **1985**, *23*, 4. (b) Trofimenko, S. *Inorg. Chem.* **1969**, *8*, 2675. (c) Drane, A. S.; McCleverty, J. A. *Polyhedron* **1983**, *2*, 53.

Table 1. ^{1}H NMR and Mass Spectrometric Data for the Ligands

	^{1}H NMR data				
ligand	pyridyl H^2/H^6	pyridyl H^3/H^5	vinyl	phenyl	EI-MS (*m/z*)
o-**L**^{2}-**A**	8.61 (4H, d)^a	7.38 (4H, d)^a	7.64 (2H, d)^b 6.93 (2H, d)	7.62 (2H, m) 7.38 (2H, m)	284
m-**L**^{2}-**A**	8.60 (4H, d)	7.39 (4H, d)	7.33 (2H, d) 7.07 (2H, d)	7.69 (1H, br s) 7.51 (2H, m) 7.43 (1H, m)	284
L^3-**A**	8.63 (6H, d)	7.42 (6H, d)	7.37 (3H, d) 7.14 (3H, d)	7.67 (3H, s)	387
L^4-**A**	8.57 (8H, d)	7.36 (8H, d)	7.58 (4H, d) 6.98 (4H, d)	7.79 (2H, s)	490
o-**L**^{2}-**B**	8.62 (4H, d)	7.39 (4H, d)		7.62 (2H, m) 7.40 (2H, m)	280
m-**L**^{2}-**B**	8.63 (4H, d)	7.39 (4H, d)		7.76 (1H, td, $J = 1.2, 0.7$ Hz) 7.57 (2H, dd, $J = 7.5, 1.2$ Hz) 7.41 (1H, td, $J = 7.5, 0.7$ Hz)	280
p-**L**^{2}-**B**	8.63 (4H, d)	7.39 (4H, d)		7.57 (4H, s)	280
L^3-**B**	8.61 (6H, d)	7.35 (6H, d)		7.71 (3H, s)	381
L^4-**B**	8.66 (8H, d)	7.40 (8H, d)		7.86 (2H, s)	482

^{a} Coupling constants for AB doublets on pyridyl rings all lie in the region 4.5–6 Hz. ^{b} Coupling constants for *trans-* double bonds are all approximately 16 Hz.

Table 2. Elemental Analyses and Percentage Yields for the New Ligands

	elem anal.^{a}			yield
compound	% C	% H	% N	(%)
o-**L**^{2}-**A**	84.2 (84.5)	5.7 (5.7)	9.7 (9.9)	80
m-**L**^{2}-**A**	84.0 (84.5)	5.6 (5.7)	9.6 (9.9)	77
L^3-**A**	83.5 (83.7)	5.4 (5.5)	11.0 (10.8)	60
L^4-**A**	83.0 (83.3)	5.5 (5.3)	11.1 (11.4)	45
o-**L**^{2}-**B**·MeOH	80.6 (80.8)	5.1 (5.1)	8.2 (9.0)	29
m-**L**^{2}-**B**·H_2O	80.0 (80.4)	4.4 (4.7)	8.7 (9.4)	25
p-**L**^{2}**B**·0.5MeOH	83.1 (83.0)	4.6 (4.7)	9.3 (9.5)	15
L^3-**B**	84.8 (85.0)	4.1 (4.0)	11.0 (11.0)	58
L^4-**B**	81.7 (81.7)	3.9 (4.3)	10.9 (10.9)	53

^{a} Expected values in parentheses.

only by the availability of polybrominated aromatics as starting materials, and these simple one-pot syntheses may be contrasted with the multistep procedures necessary for L^1 and L^2. Ligand *p*-**L**^{2}-**A** was prepared in earlier work by condensation of two equivalents of 4-picoline with benzene-1,4-dicarboxaldehyde:[3b] the Heck method is better, giving a higher yield and only requiring one reaction step rather than two. The yields of the **A**-series ligands varied from good to excellent (up to 80%), and the products were generally isolated sufficiently pure so that chromatographic workup was not necessary. The yields of some of the **B**-series ligands were sometimes lower and the crude products required more careful chromatographic purification. Other workers performing Heck reactions with ethynyl-based rather than vinyl-based starting materials have likewise on occasion obtained only moderate yields.[11a] The poor yields of *o-*, *m-* and *p*-**L**^{2}-**B** are largely due to the fact that they are difficult to separate chromatographically from other byproducts, and are waxy solids that do not crystallize well: it is likely that the actual yield is much higher than the yield of isolated material. The less soluble ligands **L**^{3}-**B** and **L**^{4}-**B** in contrast could be obtained in quite good yields (50–60%) because their higher crystallinity and lower solubility makes purification much easier. The Heck reaction has recently been popular for the preparation of extensively conjugated aromatic systems in which several phenyl rings are attached to a central core *via* unsaturated linkages,[11] but the ligands described in this paper represent the first extension of the method to polynucleating pyridyl-based analogues.[11f]

Complex Syntheses. [Mo(NO)Tp*Cl_2] readily undergoes displacement of one chloride by pyridine-based ligands, accompanied by a one-electron reduction, to give neutral 17-electron complexes of the type [Mo(NO)Tp*Cl(py)] (**Mo**-py) where **Mo** denotes the {Mo(NO)Tp*Cl} fragment and py denotes a pyridine or substituted pyridine.[3b,12] We prepared complexes of our new ligands in the same way, attaching paramagnetic **Mo** groups to some or all of the pyridyl termini. We found that particularly for the **B**-series ligands forcing conditions (prolonged reaction times and large excesses of the [Mo(NO)Tp*Cl_2] starting material) were necessary for three reasons: (i) the pyridyl groups seem to be much less nucleophilic than monodentate pyridines, and the rate of complex formation is therefore slower; (ii) with the ter- and tetradentate ligands it becomes successively more difficult to attach metal fragments as the binding sites are used up; (iii) the starting material [Mo(NO)Tp*Cl_2] has a tendency to react with traces of air and/or moisture to form [{Mo(NO)Tp*Cl}$_2$(μ−O)]. The reactions could be conveniently followed by TLC (silica, CH_2Cl_2/THF in variable proportions) and additional [Mo(NO)Tp*Cl_2] added or the reaction time lengthened as necessary until all of the free ligand was consumed. Even so, partially complexed species were obtained, particularly with the **B**-series ligands; for example with **L**^{4}-**B**, not only were the expected mono-, di-, tri- and tetranuclear complexes isolated, but also all three isomers of the dinuclear complex were obtained with the two **Mo** fragments coordinated in an *ortho*, *meta*, or *para* arrangement to two of the four pyridyl binding sites. These have been tentatively identified on the basis of their electrochemical properties (see later) since they are indistinguishable by other spectroscopic means. Similarly, with the dinucleating **B**-series ligands both mono- and binuclear complexes were isolated.

The mixtures of products could be separated very effectively by gradient elution on a silica column. Those complexes in which all pyridyl binding sites are coordinated to **Mo** fragments

---

(11) (a) Kondo, K.; Yasuda, S.; Sakaguchi, T.; Miya, M. *J. Chem. Soc., Chem. Commun.* **1995**, 55. (b) Boese, R.; Green, J. R.; Mittendorf, J.; Mohler, D. L.; Vollhardt, K. P. C. *Angew. Chem., Int. Ed. Engl.* **1992**, *31*, 1643. (c) Diercks, R.; Armstrong, J. C.; Boese, R.; Vollhardt, K. P. C. *Angew. Chem., Int. Ed. Engl.* **1986**, *25*, 268. (d) Meier, H. *Angew. Chem. Int. Ed. Engl.* **1992**, *31*, 1399 and refs. therein. (e) Diederich, F.; Philp, D.; Seiler, P. *J. Chem. Soc., Chem. Commun.* **1994**, 205. (f) An alternative synthesis of **L**^{3}-**B** has been simultaneously developed by another group: Anderson, H. L.; Walter, C. J.; Vidal-Ferran, A.; Hay, R. A.; Lowden, P. A.; Sanders, J. K. M. *J. Chem. Soc., Perkin Trans.*, in press.

(12) Das, A.; Jeffery, J. C.; Maher, J. P.; McCleverty, J. A.; Schatz, E.; Ward, M. D.; Wollermann, G. *Inorg. Chem.* **1993**, *32*, 2145.

Table 3. Analytical, Mass Spectrometric, and Yield Data for the New Complexes

complex	elem anal.[a] % C	% H	% N	FAB-MS data[a,b] M$^+$	{M − Cl}$^+$	{M − **Mo**}$^+$	{M − **Mo** − Cl}$^+$	yield/% (THF/%)[c]
Mo$_2$(*o*-L^2-A)	49.5 (50.0)	5.0 (5.0)	18.5 (18.7)	1202 (1202)	1167 (1166)	744 (744)	709 (709)	50 (2)
Mo$_2$(*m*-L^2-A)	50.5 (50.0)	5.0 (5.0)	18.4 (18.7)	1202 (1202)	1166 (1166)	744 (744)	709 (709)	55 (2)
Mo(L^3-A)	59.5 (59.6)	4.9 (5.1)	16.3 (16.6)	847 (847)	812 (812)			10 (50)
Mo$_2$(L^3-A)	52.9 (52.5)	5.1 (5.0)	17.9 (18.3)	1304 (1305)		847 (847)	812 (812)	10 (10)
Mo$_3$(L^3-A)	48.9 (49.0)	5.0 (5.0)	18.7 (19.1)	1763 (1763)		1304 (1305)	1270 (1270)	45 (2)
Mo$_4$(L^4-A)	48.5 (48.6)	5.4 (4.9)	19.1 (19.3)			1867 (1866)	1832 (1831)	15 (2)
Mo(*o*-L^2-B)	56.2 (56.9)	4.8 (4.6)	17.2 (17.1)	740 (740)	705 (705)			34 (2.5)
Mo$_2$(*o*-L^2-B)	49.5 (50.2)	4.9 (4.7)	18.2 (18.7)	1197 (1198)	1163 (1163)	740 (740)	705 (705)	12 (0.5)
Mo(*m*-L^2-B)	56.2 (56.9)	4.6 (4.6)	17.1 (17.1)	740 (740)	705 (705)			26 (2.5)
Mo$_2$(*m*-L^2-B)	50.3 (50.2)	4.7 (4.7)	18.4 (18.7)	1199 (1198)		740 (740)	706 (705)	11 (1)
Mo(*p*-L^2-B)	56.9 (56.9)	4.7 (4.6)	16.8 (17.1)	740 (740)	705 (705)			42 (2)
Mo$_2$(*p*-L^2-B)	49.8 (50.2)	4.8 (4.7)	18.3 (18.7)	1197 (1198)	1164 (1163)	740 (740)	705 (705)	22 (2)
Mo(L^3-B)	59.9 (60.1)	4.6 (4.4)	16.6 (16.7)	841 (841)	806 (806)			45 (50)
Mo$_2$(L^3-B)	52.8 (52.7)	4.9 (4.6)	17.8 (18.3)	1296 (1299)	1263 (1263)	841 (841)	806 (806)	34 (10)
Mo$_3$(L^3-B)	49.2 (49.2)	4.8 (4.6)	18.7 (19.1)	1757 (1757)	1722 (1722)			14 (1)
Mo(L^4-B)	62.7 (62.5)	4.8 (4.3)	15.8 (16.4)	942 (942)	907 (907)			16 (50)
***o*-Mo$_2$(L^4-B)**	54.6 (54.9)	4.4 (4.5)	17.4 (18.0)	1400 (1400)	1364 (1365)	942 (942)	907 (907)	9 (25)
***m*-Mo$_2$(L^4-B)**	53.7 (54.9)	4.7 (4.5)	17.9 (18.0)	1400 (1400)	1365 (1365)	942 (942)	907 (907)	5 (10)
***p*-Mo$_2$(L^4-B)**	54.5 (54.9)	4.8 (4.5)	17.6 (18.0)	1399 (1400)	1364 (1365)	942 (942)	907 (907)	5 (10)
Mo$_3$(L^4-B)	51.0 (51.1)	4.8 (4.6)	18.4 (18.8)	1860 (1858)	1822 (1823)	1399 (1400)	1364 (1365)	10 (2.5)
Mo$_4$(L^4-B)	48.4 (48.7)	4.8 (4.6)	19.5 (19.3)	2315 (2317)				26 (1)

[a] Expected values in parentheses. [b] The most intense peak of the (broad) isotope cluster is given in each case. [c] The % THF figure in parentheses is the proportion of THF in CH_2Cl_2 required for column chromatography on silica (see Experimental Section).

Table 4. Electrochemical and UV/vis Spectroscopic Data for the New Complexes

complex	electrochem data ($E_{1/2}$)[a] oxidns	redns	$\Delta E_{1/2}$/mV	UV/vis spectral data[d] λ_{max}/nm (ϵ/M^{-1} cm^{-1})
Mo$_2$(*o*-L^2-A)	+0.05 (90, 2e)	−1.71 (150, 1e), −1.88 (170, 1e)	170	304 (32), 345 (25), 575 (2.8)
Mo$_2$(*m*-L^2-A)	+0.04 (80, 2e)	−1.78 (1e), −1.86 (1e)[b]	60	286 (23), 324 (40), 426 (5.8), 489 (3.8), 572 (2.8)
Mo$_2$(*p*-L^2-A)	+0.05 (70, 2e)	−1.66 (60, 1e), −1.82 (80, 1e)	160	281 (16), 374 (51), 437 (sh), 519 (7.3)
Mo(L^3-A)	+0.04 (100, 1e)	−1.77 (120, 1e)	N/A	314 (65), 428 (3.0), 496 (2.4), 567 (1.9)
Mo$_2$(L^3-A)	+0.03 (90, 2e)	−1.78 (190, 2e)	*c*	324 (71), 426 (6.4), 494 (4.9), 565 (4.1)
Mo$_3$(L^3-A)	+0.02 (100, 3e)	−1.79 (230, 3e)	*c*	324 (77), 495 (6.4), 564 (5.7)
Mo(*o*-L^2-B)	+0.07 (110, 1e)	−1.71 (130, 1e)	N/A	281 (33), 559 (2.8)
Mo$_2$(*o*-L^2-B)	+0.08 (90, 2e)	−1.66 (90, 1e), −1.78 (90, 1e)	120	284 (sh), 291 (44), 563 (5.4)
Mo(*m*-L^2-B)	+0.06 (100, 1e)	−1.75 (110, 1e)	N/A	283 (43), 300 (44), 549 (2.8)
Mo$_2$(*m*-L^2-B)	+0.04 (150, 2e)	−1.79 (200, 2e)	*c*	285 (sh), 299 (50), 312 (48), 552 (5.4)
Mo(*p*-L^2-B)	+0.02 (180, 1e)	−1.77 (180, 1e)	N/A	285 (sh), 333 (42), 482 (1.9), 556 (2.7)
Mo$_2$(*p*-L^2-B)	+0.06 (170, 2e)	−1.68 (1e), −1.81 (1e)[b]	130	283 (26), 340 (38), 490 (3.9), 563 (6.0)
Mo(L^3-B)	+0.06 (120, 1e)	−1.73 (160, 1e)	N/A	284 (63), 293 (59), 302 (65), 556 (2.6)
Mo$_2$(L^3-B)	+0.05 (160, 2e)	−1.75 (200, 2e)	*c*	285 (73), 295 (75), 302 (79), 556 (5.4)
Mo$_3$(L^3-B)	+0.05 (120, 3e)	−1.73 (200, 3e)	*c*	286 (sh), 295 (81), 302 (82), 559 (7.5)
Mo(L^4-B)	0.00 (100, 1e)	−1.56 (110, 1e)	N/A	312 (97), 532 (2.8), 581 (3.2)
***o*-Mo$_2$(L^4-B)**	+0.08 (90, 2e)	−1.51 (90, 1e), −1.73 (90, 1e)[b]	220	313 (≈80), 535 (sh), 583 (≈4)[e]
***m*-Mo$_2$(L^4-B)**	+0.08 (100, 2e)	−1.53 (120, 1e), −1.68 (130, 1e)	150	
***p*-Mo$_2$(L^4-B)**	+0.08 (150, 2e)	−1.51 (160, 1e), −1.74 (160, 1e)	230	
Mo$_3$(L^4-B)	+0.07 (120, 3e)	−1.47 (110, 1e), −1.71 (1e), −1.80 (1e)[b]	240, 90	317 (86), 535 (sh), 588 (7.4)
Mo$_4$(L^4-B)	+0.08 (100, 4e)	−1.39 (90, 1e), −1.67 (90, 1e), −1.82 (120, 2e)	280, 150	322 (100), 544 (sh), 597 (12)

[a] Electrochemical data recorded in CH_2Cl_2/0.1 M $^nBu_4PF_6$ using at Pt-bead working electrode at a scan rate of 0.2 V s^{-1}. Potentials are in volts *vs* the ferrocene/ferrocenium couple (Fc/Fc$^+$). The figures in parentheses are the peak–peak separation ΔE_p for the symmetric waves, and the number of electrons involved. [b] ΔE_p value not available as two or more waves were partially overlapping and not fully resolved by cyclic voltammetry; $E_{1/2}$ values therefore taken from Osteryoung square-wave voltammograms. [c] Separation between reductions could not be measured as the processes are not resolved but give one broad combined wave. [d] UV/vis spectra recorded in CH_2Cl_2. [e] The three isomers of **Mo$_2$-(L^4-B)** have essentially identical spectra.

are relatively nonpolar and elute first: free pyridyl groups increase the retention on silica and therefore require more polar solvents. For the **A**-series ligands in contrast the intermediate complexes were less in evidence, and we only isolated and characterised the intermediate complexes for **L^3-A**: although intermediate complexes of lower nuclearity were evident by TLC for the bidentate and tetradentate ligands, they were not isolated and characterised.

Characterisation data for the complexes are in Tables 3 and 4. All of the complexes exhibited intense bands in the UV region of their electronic spectra, which are π–π^* transitions of both the Tp* ligands and the highly conjugated bridging ligands, and weaker transitions in the visible region which, by comparison with other related complexes,[3b,12] are molybdenum-to-pyridine charge-transfer bands. In addition, all complexes gave $\nu_{NO} = 1608 \pm 2$ cm^{-1} and $\nu_{BH} = 2553 \pm 1$ cm^{-1} in their IR spectra.

Electrochemical Properties. All complexes of the type [Mo(NO)Tp*Cl(pyr)] undergo a chemically reversible one-electron oxidation to the 16-electron cation, and a one-electron reduction to the 18-electron anion.[3b,12] The oxidation potentials are not sensitive to substitutents on the pyridine ligands and generally occur at *ca.* +0.1 V *vs* the ferrocene/ferrocenium couple (Fc/Fc$^+$), and for this reason we believe that they are primarily metal-centerd. The reductions, in contrast, are very sensitive to the nature of remote electron-withdrawing or electron-

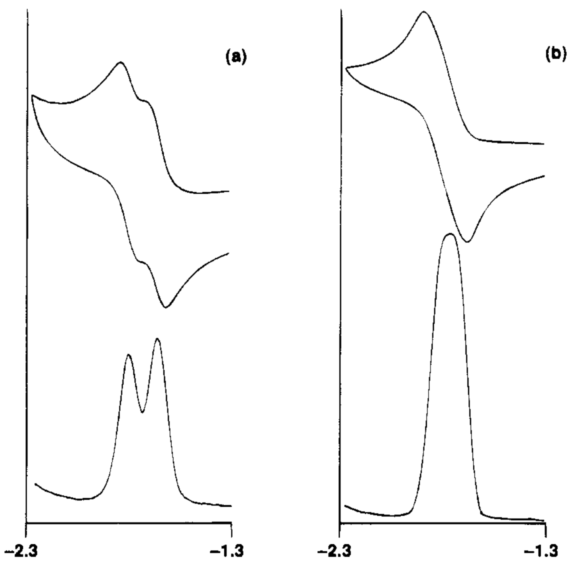

Figure 2. Reductive cyclic and square-wave voltammograms of (a) Mo_2-(*o*-**L^2-B**) and (b) Mo_2-(***m*-L^2-B**), showing how the redox separation $\Delta E_{1/2}$ varies with ligand substitution pattern.

donating substituents on the pyridine ligand, which suggests that they are partly ligand-based. A consequence of this is that in dinuclear complexes with ligands such as 4,4′-bipyridine there is an extremely strong electrochemical interaction between the two reductions—$\Delta E_{1/2}$ = 765 mV in **Mo_2**(4,4′-bipy)—but not between the oxidations, which remain virtually coincident. The magnitude of this electrochemical splitting between the 17 e/18 e couples, even across long bridging ligands, makes the {Mo-(NO)Tp*Cl} fragment ideal for examining the relative abilities of bridging ligands at transmitting electronic interactions between metal centers.

The electrochemical properties of the complexes are summarized in Table 4. In general all of the processes are chemically reversible on the cyclic voltammetric timescale since the waves in cyclic voltammograms are symmetric. The peak–peak separations ΔE_p for the resolved one-electron processes are often larger than the ideal 59 mV, due to a combination of slightly slow electron-transfer kinetics and uncompensated solution resistance in CH_2Cl_2: this is typical for these complexes. Since we isolated more complexes with the **B**-series ligands we shall use these as a basis for the discussion of the electrochemical properties, but the same arguments apply to the **A**-series. For the five mononuclear complexes the first reduction potentials (the 17-electron/18-electron couple) vary: in particular, the reduction of **Mo(L^4-B)** ($E_{1/2}$ = −1.55 V *vs* Fc/Fc$^+$) is at a considerably less cathodic potential than the first reductions of **Mo(L^3-B)** and the three isomers **Mo(L^2-B)** (all between −1.70 and −1.75 V). This may be ascribed to the more extensive conjugated network of the pyridyl ligand **L^4-B** and further reinforces our suggestion that the reductions are partially ligand-based.

Within the series of three dinucleating ligands the expected variation of $\Delta E_{1/2}$ with substitution pattern is clear: for the *ortho*- and *para*-substituted dinuclear complexes there is a significant interaction [$\Delta E_{1/2} \approx$ 130 mV], whereas for the *meta*-substituted complex the two reductions are much closer together and cannot be resolved, giving one rather broad wave in both cyclic and square-wave voltammograms (Figure 2). Ligand ***m*-L^2-B** is therefore a much poorer mediator of electrochemical interactions than the *ortho*- and *para*-substituted analogues. We have observed this before[12] and it confirms that the electrochemical interaction is transmitted primarily through the conjugated π-system. The same is true of the **A**-series of bidentate ligands. For the three isomeric dinuclear complexes **Mo_2(L^4-B)**, in which two pyridyl sites of the tetradentate ligand **L^4-B** are coordinated to **Mo** fragments and two are free, the redox separations $\Delta E_{1/2}$ are much higher than in the corresponding dinuclear complexes of *o*-, *m*-, and *p*-**L^2-B**. This provides a basis for identifying the three complexes, since the ΔE_p separations tend to vary in the order *para* > *ortho* > *meta*. Thus the value of $\Delta E_{1/2}$ between two *meta*-oriented **Mo** fragments of *m*-**Mo_2(L^4-B)** is 160 mV, in contrast to the near-coincidence of the reductions in **Mo_2**(*m*-**L^2-B**); likewise, the $\Delta E_{1/2}$ values between the *ortho*- and *para*-oriented **Mo** fragments are both *ca.* 230 mV when the metals are attached to **L^4-B** but both 130 mV when the metals are attached to *o*- or *p*-**L^2-B**. An explanation for this may be that the two additional conjugated arms in the dinuclear complexes **Mo_2(L^4-B)**, although not directly involved in coordination to metals, lower the energy of the π^* orbitals of the bridging ligand **L^4-B** and therefore improve the d(π)–p(π^*) overlap between the **Mo** centers and the ligand framework through which the interaction is transmitted. Similarly, we would expect the redox splitting $\Delta E_{1/2}$ in **Mo_2(L^3-B)** to be larger than that in **Mo_2**(*m*-**L^2-B**), however it is not possible to tell as the two reduction processes still overlap and cannot be resolved.

Understanding the interactions in the dinuclear complexes helps to understand the electrochemical behaviour of the trinuclear and tetranuclear species. In the trinuclear complexes **Mo_3(L^3-A)** and **Mo_3(L^3-B)** the three reductions are virtually coincident, giving a single broad wave in both cyclic and square-wave voltammograms, which is to be expected due to the *meta* substitution pattern. Although shoulders are visible, confirming the presence of processes at slightly different potentials, individual $E_{1/2}$ values cannot be extracted. However in the tetranuclear complex **Mo_4(L^4-B)** the voltammograms are much more clearly resolved (Figure 3). The first two one-electron reductions are separated by $\Delta E_{1/2}$ = 280 mV; these are followed by two coincident reductions at a potential 150 mV more negative than the second. The large redox separations that we see here may again be ascribed to the low energy of the π^* orbital of the highly conjugated ligand, which results in particularly effective d(π)–p(π^*) overlap with the metals. The first reduction could of course occur on any of the metal centers. From the magnitude of the separation between the first and second reductions, and on electrostatic grounds, it seems reasonable to assign the second reduction to the **Mo** center *para* to the first one. The third and fourth **Mo** centers then apparently reduce nearly together, which is unexpected and for which we have no explanation yet. In the trinuclear complex **Mo_3(L^4-B)**, for which only one isomer is possible, the three reductions are all resolved with redox separations $\Delta E_{1/2}$ of 240 mV between the first and second reductions, and 90 mV between the second and third. We found that **Mo_4(L^4-A)** did not give reliable electrochemical data since it is prone to partial decomposition in solution, by detachment of one or more **Mo** fragments. Of all the complexes we prepared this alone did not give a molecular ion by FAB mass spectrometry, and the EPR spectrum (see later) also confirmed that it is unstable in solution. Consequently, electrochemical data are not given.

Finally we note that comparison of the two sets of dinucleating ligands show that the series **A** ligands give slightly stronger interactions between the metals than the series **B** ligands; for example the separation $\Delta E_{1/2}$ between the reductions of ***p*-L^2-A** is 160 mV in contrast to 130 mV for ***p*-L^2-B.** It is perhaps unexpected that triple bonds make poorer "molecular wires" than double bonds, but this is consistent with our earlier work

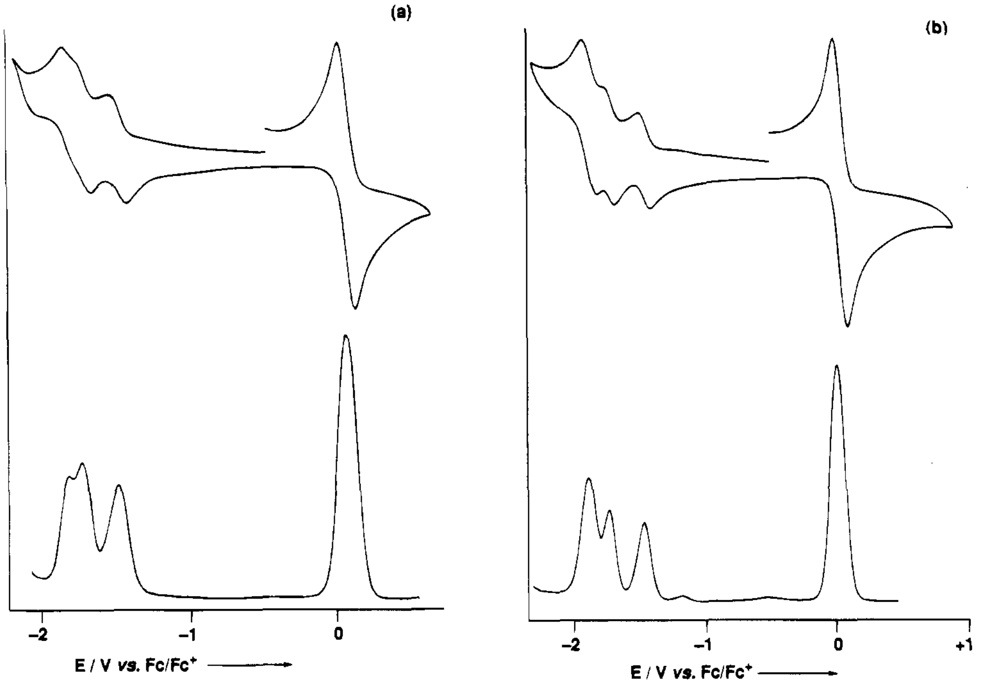

Figure 3. Cyclic and square-wave voltammograms of (a) $Mo_3(L^4\text{-}B)$ and (b) $Mo_4(L^4\text{-}B)$. Note the single multielectron oxidation wave in each case.

where we observed that 1,2-bis(4-pyridyl)ethyne as a bridging ligand between Mo centers gave a slightly smaller $\Delta E_{1/2}$ value than did *trans*-1,2-bis(4-pyridyl)ethane.[3b]

EPR Spectra. In addition to their favorable electrochemical properties, complexes containing the {Mo(tp*)(NO)Cl} fragment (a one-electron paramagnet) are ideal for examining magnetic exchange interactions by EPR spectroscopy due to the clear, well-resolved sextet hyperfine coupling pattern of the spin-active Mo nuclei ($I = {}^5/_2$). If two Mo fragments are magnetically coupled, provided the modulus of J (the spin−spin exchange interaction) is much greater than A_{Mo}, the hyperfine interaction—a condition which is easily fulfilled for all but the weakest exchange interactions[12]—then a spectrum appears in which both electrons are apparently coupled to both metal centers. The separation between hyperfine signals is halved (typically, from *ca.* 5 to *ca.* 2.5 mT) and an 11-fold multiplet arises from coupling to two equivalent $I = {}^5/_2$ nuclei. We have observed spectra of this type in many bridged-dinuclear complexes containing Mo fragments,[3a,12,13] and describe here how this can be extended to the detection of spin-exchange interactions between three and four metal centers.

The solution EPR spectra of the mono-, di-, and trinuclear complexes of L^3-**B** are given in Figure 4. All are centered at $g_{iso} = 1.979(1)$. The spectrum of $Mo(L^3\text{-}B)$ (Figure 4a) is entirely typical of mononuclear molybdenum complexes, consisting of a singlet (component **A**, from ≈75% of the Mo nuclei which have $I = 0$) and a sextet (component **B**, from ≈25% of the Mo nuclei with $I = {}^5/_2$) with an average separation between hyperfine signals of 4.8 mT. The spectrum of $Mo_2(L^3\text{-}B)$ (Figure 4b) is characteristic of two exchange-coupled molybdenum centers, with a singlet (**A**, from the $I = 0$, $I = 0$ nuclear spin combination), a 1:1:1:1:1:1 sextet (**B**, from the $I = 0$, $I = {}^5/_2$ spin combination) and a 1:2:3:4:5:6:5:4:3:2:1 11-fold multiplet (component **C**, from the $I = {}^5/_2$, $I = {}^5/_2$ spin combination) superimposed.[3a,12,13] The hyperfine separation in both the sextet and 11-fold multiplet is 2.4 mT, half the value of the mononuclear complexes. The spectrum of $Mo_3(L^3\text{-}B)$ (Figure 4c) displays the features that are expected if all three unparied spins are undergoing exchange interactions, with (in this case) an equivalent interaction between each pair of spins in the equilateral triangle. The signal shows coupling to all three molybdenum nuclei, giving a superposition of a singlet (nuclear spin combination 0, 0, 0; 42% probability, component **A**), a sextet (0, 0, ${}^5/_2$; 42% probability, component **B**), an 11-fold multiplet (0, ${}^5/_2$, ${}^5/_2$; 14% probability, component **C**) and a 16-fold multiplet (${}^5/_2$, ${}^5/_2$, ${}^5/_2$; *ca.* 2% probability, component **D**). The 16-fold multiplet **D** is predicted to have an intensity pattern of 1:3:6:10:15:21:25:27:27:25:21:15:10:6:3:1. Only the outer components are visible, on the low-field side of the spectrum, and they are of course very weak, but their relative intensities are approximately as expected. The outer components of all four sets of signals **A**−**D** are visible and labeled on the spectra in Figure 4, and in the three sets which show hyperfine coupling (6-, 11-, and 16-fold multiplets, **B**−**D** respectively) the separation between adjacent components is 1.6 mT, exactly one-third of the value found in the spectra of mononuclear complexes. The other trinuclear complexes $Mo_3(L^3\text{-}A)$ and $Mo_3(L^4\text{-}B)$ give essentially identical spectra. In the case of $Mo_3(L^4\text{-}B)$ the three pairwise interactions are nonequivalent (one *ortho* interaction, one *meta*, and one *para*) and hence may have different values of J. Provided however that the criterion $|J| \gg A_{Mo}$ is met for each interaction, then a spectrum of this type is to be expected.

The spectrum of $Mo_4(L^4\text{-}B)$ (Figure 5) shows that magnetic exchange is occurring between *all four* unpaired electrons. The spin combinations [0, 0, 0, 0; 32% probability], [0, 0, 0, ${}^5/_2$; 42%], [0, 0, ${}^5/_2$, ${}^5/_2$; 21%], [0, ${}^5/_2$, ${}^5/_2$, ${}^5/_2$; *ca.* 4.6%] and [${}^5/_2$, ${}^5/_2$, ${}^5/_2$, ${}^5/_2$; *ca.* 0.4%] give five superimposed signals of multiplicity 1, 6, 11, 16, and 21 (components **A**−**E** respectively, following the labelling scheme above); the expected intensity pattern for the 21-fold multiplet **E** is 1:4:10:20:35:56:80:104:125:140:146:140:125:104:80:56:35:20:10:4:1. The first four sets of signals are clearly in evidence, with the outer components of the 16-fold multiplet **D** resolved. The outer components of the 21-fold multiplet **E** are barely distinguishable from the background

---

(13) (a) Cook, R.; Maher, J. P.; McCleverty, J. A.; Ward, M. D.; Wlodarczyk, A. *Polyhedron* **1993**, *12*, 2111. (b) Maher, J. P.; McCleverty, J. A.; Ward, M. D.; Wlodarczyk, A. *J. Chem. Soc., Dalton Trans.* **1994**, 143.

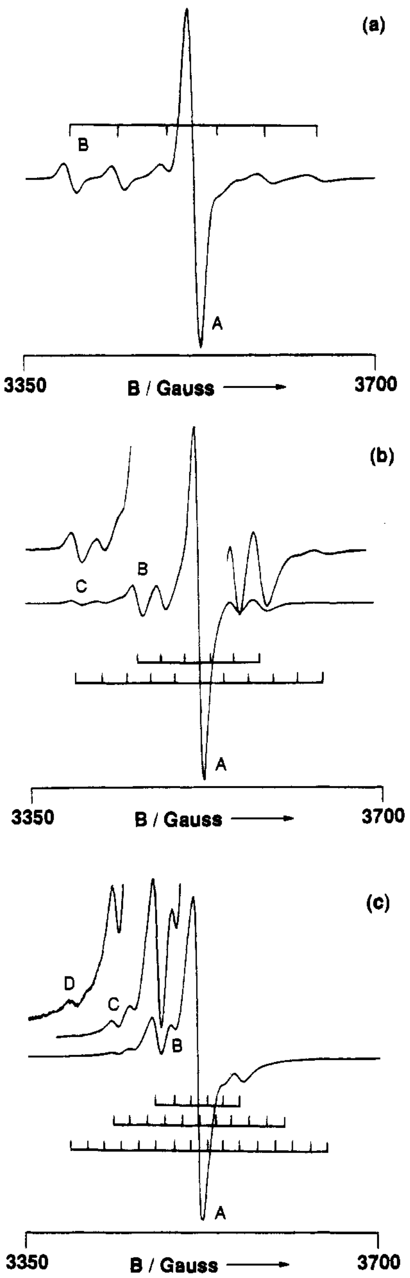

Figure 4. Solution EPR spectra of (a) $\mathbf{Mo(L^3\text{-}B)}$, (b) $\mathbf{Mo_2(L^3\text{-}B)}$, and (c) $\mathbf{Mo_3(L^3\text{-}B)}$ in CH_2Cl_2 at room temperature. The labels A–D denote the different sets of hyperfine multiplets (see text).

noise, even in a spectrum comprising several hundred accumulations: the *total* intensity of this multiplet is *ca.* 0.4% of the entire spectrum, and its outermost component is 1/1296 of the intensity of the multiplet, so the outermost hyperfine component of the 21-fold multiplet is just 0.001% of the intensity of the central singlet. However the separation between adjacent hyperfine components in all of the resolved multiplets is now 1.2 mT, one-fourth of the value found in the spectra of mononuclear complexes. The appearance of the spectrum again implies that all six pairwise exchange interactions (two *ortho*, two *meta* and two *para*) between the four paramagnetic metal centers fulfil the criterion $|J| \gg A_{Mo}$. It is apparent from these examples that the hyperfine coupling to molybdenum nuclei affords a particularly useful probe of magnetic exchange. The other tetranuclear complex, $\mathbf{Mo_4(L^4\text{-}A)}$, gave a similar solution EPR spectrum when the solution was freshly prepared, but after about an hour additional signals arising from mononuclear molybdenum fragments became apparent due to partial decomposition of the complex.

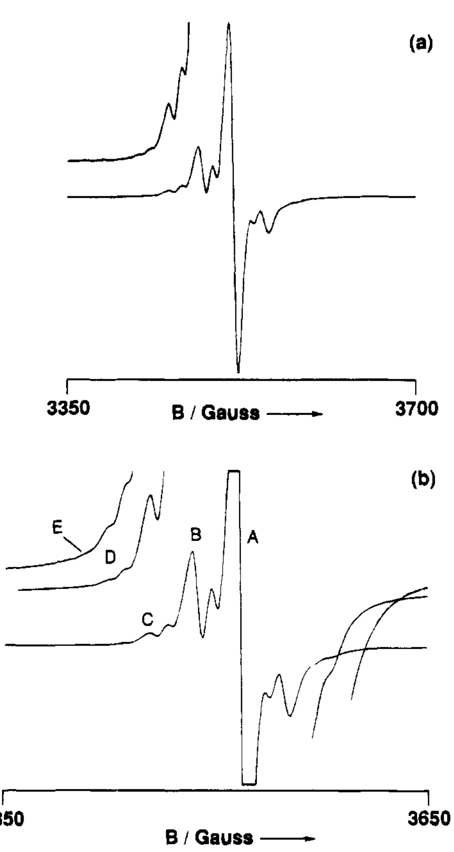

Figure 5. Solution EPR spectra of $\mathbf{Mo_4(L^4\text{-}B)}$ in CH_2Cl_2 at room temperature. Spectrum a is on the same scale as the spectra in Figure 4; spectrum b is an expansion.

Although they have been the subject of theoretical investigations,[14,15] the study of magnetic exchange interactions in triangular systems[16–20] is much sparser than in linear three-center systems,[21] primarily for synthetic reasons. Some triangular organic triradicals have been examined.[16] The principal inorganic systems are the oxo-centered trinuclear carboxylates[17] and a series of hydroxo-centered Cu(II) trimers with bridging ligands around the edges of the triangle,[18] which have been characterized by low temperature susceptibility studies but not EPR spectroscopy. A vanadyl pyrophosphate trimer has been

---

(14) Hudson, A.; Luckhurst, G. R. *Mol. Phys.* **1967**, *13*, 409.

(15) (a) Griffith, S. J. *Struct. Bonding (Berlin)* **1972**, *10*, 87. (b) Yamaguchi, K. *Chem. Phys. Lett.* **1975**, *30*, 288. (c) Goodyear, G.; Stratt, R. M. *J. Am. Chem. Soc.* **1993**, *115*, 10452.

(16) (a) Brickman, J.; Kothe, G. *J. Chem. Phys.* **1973**, *59*, 2807. (b) Nowak, C.; Kothe, G.; Zimmermann, H. *Ber. Bunsen-Ges. Phys. Chem.* **1974**, *78*, 265. (c) Kirste, B.; Grimm, M.; Kurreck, H. *J. Am. Chem. Soc.* **1989**, *111*, 109. (d) Veciana, J.; Rovira, C.; Ventosa, N.; Crespo, M. I.; Palacio, F. *J. Am. Chem. Soc.* **1993**, *115*, 57. (e) Rajca, A.; Utamapanya, S. *J. Am. Chem. Soc.* **1993**, *115*, 2396.

(17) (a) Vincent, J. B.; Chang, H.-R.; Folting, K.; Huffman, J. C.; Christou, G.; Hendrickson, D. N. *J. Am. Chem. Soc.* **1987**, *109*, 5703. (b) Dziobowski, C. T.; Wroblewski, J. T.; Brown, D. B. *Inorg. Chem.* **1981**, *20*, 671. (c) Dziobowski, C. T.; Wroblewski, J. T.; Brown, D. B. *Inorg. Chem.* **1981**, *20*, 684. (d) Schriempf, J. T.; Friedberg, S. A. *J. Chem. Phys.* **1964**, *40*, 296.

(18) (a) Beckett, R.; Colton, R.; Hoskins, B. F.; Martin, R. L.; Vince, D. G. *Aust. J. Chem.* **1969**, *22*, 2527. (b) Butcher, R. J.; O'Connor, C. J.; Sinn, E. *Inorg. Chem.* **1981**, *20*, 537. (c) Ho, D. M.; Bau, R. *Inorg. Chem.* **1983**, *22*, 4079. (d) Agnus, Y.; Louis, R.; Metz, B.; Boudon, C.; Gisselbrecht, J. P.; Gross, M. *Inorg. Chem.* **1991**, *30*, 3155 and references therein.

(19) Chaudhuri, P.; Karpenstein, I.; Winter, M.; Butzlaff, C.; Bill, E.; Trautwein, A. X.; Flörke, U.; Haupt, H.-J. *J. Chem. Soc., Chem. Commun.* **1992**, 321.

(20) (a) Parker, C. C.; Reeder, R. R.; Richards, L. B.; Rieger, P. H. *J. Am. Chem. Soc.* **1970**, *92*, 5320. (b) Hasegawa, A. *J. Chem. Phys.* **1971**, *55*, 3101.

(21) See Chapter 10 of ref 3a.

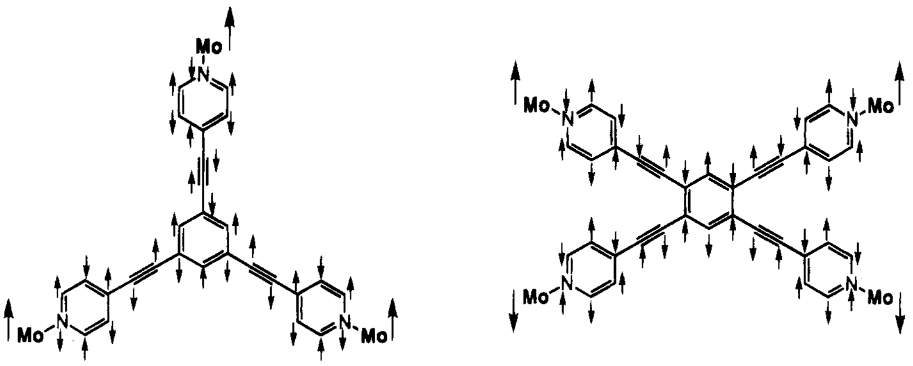

Figure 6. Prediction of the ground-states of (a) **Mo$_3$(L^3-B)** [$S = {}^3/_2$] and (b) **Mo$_4$(L^4-B)** [$S = 0$] according to the McConnell spin-polarization mechanism. The large arrows on the molybdenum atoms denote the unpaired spins; the small arrows on the atoms of the bridging ligand denote the direction of polarization of the electron cloud.

desribed which gives a 22-line EPR spectrum but whose structure is uncertain.[20] **Mo$_3$(L^3-A)** and **Mo$_3$(L^3-B)** are therefore rare examples of well-characterized triangular complexes, and the first where three-center magnetic exchange is clear from the EPR spectra.

The arrangement of four magnetic centers in a rectangle is particularly rare: many magnetically interesting tetranuclear complexes are known, but they generally have different topologies (three magnetic centers linked in a triangular arrangement around a central fourth one, linear chains, and cubanes).[21] Complexes **Mo$_4$(L^4-A)** and **Mo$_4$(L^4-B)** are therefore unusual examples of this type of structure, as well as being the first examples of complexes where magnetic exchange between four metal centers can be unequivocally established by EPR spectroscopy.

In the absence of close contacts between the paramagnetic centers which would allow direct overlap of magnetic orbitals, the exchange interaction is likely to be propagated *via* a McConnell-type spin-polarization of the bridging ligand, in which an unpaired electron on one atom polarises the electron cloud on the adjacent atom in the opposite sense.[22] This results in an alternation of the spin density of atoms in the bridge and allows the sign of J to be predicted. If this mechanism is operative we might expect, for example, that the triangular trinuclear complexes have $S = {}^3/_2$ ground states (ferromagnetic exchange) and that the rectangular tetranuclear complexes have $S = 0$ ground states (antiferromagnetic exchange) as depicted in Figure 6. We are currently investigating the low-temperature magnetic properties of the complexes and these will be the subject of a separate report.

Acknowledgment. We thank the EPSRC for post-doctoral grants (to A.J.A. and A.M.W.C.T.) and for a grant to purchase the EPR spectrometer.

IC9504856

---

[22] (a) McConnell, H. M. *J. Chem. Phys.* **1963**, *39*, 1910. (b) See Chapter 12 of ref 3a.